https://doi.org/10.5194/egusphere-2024-2704
Preprint. Discussion started: 6 September 2024

Impacts of meteorology and emission reductions on haze pollution during the lockdown in the North China Plain: Insights from six-year simulations

Lang Liu[1,2], Xin Long[3,*] Yi Li[1,2*], Zengliang Zang[1,2], Yan Han[3], Zhier Bao[3], Yang Chen[3], Tian Feng[4], Jinxin Yang[5]

[1]College of Meteorology and Oceanography, National University of Defense Technology, Changsha, 410073, China

[2]High Impact Weather Key Laboratory of CMA, Changsha, 410073, China

[3]Research Center for Atmospheric Environment, Chongqing Institute of Green and Intelligent Technology, Chinese Academy of Sciences, Chongqing 400714, China

[4] Department of Geography & Spatial Information Techniques, Ningbo University, Ningbo, China

[5]School of Geography and Remote Sensing, Guangzhou University, Guangzhou 510006, China

Correspondence to: longxin@cigit.ac.cn, liyiqxxy@163.com

https://doi.org/10.5194/egusphere-2024-2704
Preprint. Discussion started: 6 September 2024

Abstract.

Haze events across the North China Plain (NCP) during the COVID-19 lockdown have highlighted the complexities of air quality management in the face of reduced human activity. While previous studies have focused primarily on the atmospheric chemistry processes under anomalous weather conditions, interactions between air pollutants, atmospheric chemistry, and their responses to emissions and meteorological factors remain underexplored. Here, we utilized the WRF-Chem model to assess the impact of abrupt emission reductions and meteorological conditions on $PM_{2.5}$ levels across the NCP. By comparing simulations sensitive to meteorological conditions with climatology averaged over 2015–2019 and considering the sudden decrease in anthropogenic emissions due to the lockdown, we identified significant regional disparities. In the Northern NCP (NNCP), adverse meteorological conditions negated the benefits of emission reductions, leading to a net increase in $PM_{2.5}$ levels by 30 to 60 μg m^{-3} during haze episodes. Conversely, the Southern NCP (SNCP) experienced a decrease in $PM_{2.5}$ levels attributed to favourable meteorological conditions combined with emission reductions, with decreases ranging from 20 to 40 μg m^{-3} during the same periods. Our results highlight the critical role of meteorological conditions in modulating the effects of emission reductions, particularly in regions like the NNCP, where adverse weather can significantly counteract the benefits of reduced emissions. This study provides valuable insights into the complex interactions between emissions, meteorology, and air quality, underscoring the necessity of integrated approaches that address emissions and atmospheric dynamics.

https://doi.org/10.5194/egusphere-2024-2704
Preprint. Discussion started: 6 September 2024

1 Introduction

Fine particulate matter ($PM_{2.5}$) is a critical issue for both policymakers and the general public due to its widespread presence and adverse impacts on human health(Lelieveld et al., 2018), agriculture productivity(Dong and Wang, 2023), and the Earth's radiation balance (Li et al., 2022; Yang et al., 2021). The formation and accumulation of anthropogenic $PM_{2.5}$ result from a complex interaction of emission sources, atmospheric chemical processes, and meteorological conditions (Le et al., 2020). Beyond significant local primary emissions and secondary chemical formation, stagnant meteorological conditions and regional transport significantly contribute to severe haze pollution events (Feng et al., 2020; Li et al., 2021). China has implemented a series of air quality regulations, significantly reducing anthropogenic emissions and improving air quality, particularly through reductions in $PM_{2.5}$ levels (Xiao et al., 2020; Zhang et al., 2019). For instance, the Beijing-Tianjin-Hebei (BTH) region witnessed a decline in the number of days with severe $PM_{2.5}$ pollution from 122 days in 2013 to 31 days in 2017 (Li et al., 2019). Despite these improvements, severe $PM_{2.5}$ pollution events still occur. Research has demonstrated that adverse meteorological conditions often play a dominant role in influencing $PM_{2.5}$ concentrations in North China (Le et al., 2020; Shen et al., 2024; Wang et al., 2020), frequently offsetting the positive effects of emission reductions.

The coronavirus disease 2019 (COVID-19) pandemic, which has persisted for over 4.5 years, resulted in more than 7 million deaths globally by June 2023(WHO, 2024). In response to the initial outbreak, the Chinese government enforced stringent lockdowns nationwide during the first 2 months of 2020 to limit the virus's spread (Le et al., 2020). These measures led to a sharp decline in anthropogenic emissions, particularly from the transportation sector (Liu et al., 2021; Xu et al., 2020). However, during the period from January 21 to February 16 2020, the Northern China Plain (NCP) experienced severe haze pollution, a stark contrast to other regions (Huang et al., 2021; Le et al., 2020; Wang et al., 2021). This unusual event on the NCP, occurring during a time of reduced human activity, provides a unique opportunity to study the complex interactions between atmospheric chemistry and meteorology under these exceptional conditions.

Recent research on the haze above event in China has highlighted that the unexpected regional haze formation during the COVID-19 lockdown was largely driven by complex atmospheric chemical

https://doi.org/10.5194/egusphere-2024-2704
Preprint. Discussion started: 6 September 2024

processes influenced by both emission reductions and meteorological factors(Ding et al., 2021; Li et al., 2021). Specifically, the sharp decline in NO_2 emissions during the lockdown led to elevated O_3 levels and increased night-time formation of NO_3 radicals, which boosted the atmospheric oxidation capacity and promoted the generation of secondary aerosols. Furthermore, anomalously high relative humidity during this period facilitated heterogeneous chemical reactions, further contributing to aerosol formation (Huang et al., 2021; Le et al., 2020; Ma et al., 2022)(Le et al., 2020; Huang et al., 2021; Ma et al., 2022). Once formed, these secondary aerosols were transported to monitoring stations in northern China, exacerbating local pollution levels (Lv et al., 2020). Some studies have emphasized that elevated ambient humidity is crucial in enhancing nitrate aerosols' formation efficiency—a key haze component—by influencing pH levels (Chang et al., 2020; Sun et al., 2020). In addition to these chemical interactions, the aerosol–planetary boundary layer (PBL) feedback mechanism is also believed to have significantly contributed to the haze event (Su et al., 2020). Overall, meteorological conditions influenced the formation, accumulation, and dispersion of $PM_{2.5}$ during this period. However, the precise interactions between air pollutants, atmospheric chemistry, and their responses to emissions and meteorological conditions have not been clearly determined.

In this study, we utilized the WRF-Chem model to evaluate the effects of meteorological conditions and abrupt reductions in anthropogenic emissions on $PM_{2.5}$ levels in the NCP. We addressed three key questions by simulating severe air pollution episodes during the COVID-19 lockdown: (1) How do sudden emission reductions affect $PM_{2.5}$ levels under varying meteorological scenarios? (2) What are the key drivers of $PM_{2.5}$ formation and accumulation during these emission reductions? (3) How do meteorological conditions interact with lowered emissions to shape air quality outcomes? Through this analysis, we aim to offer valuable insights into the effectiveness of short-term emission control strategies and to explore the implications of future low-emission scenarios by examining the combined effects of meteorological variations and emission reductions on $PM_{2.5}$ concentrations.

https://doi.org/10.5194/egusphere-2024-2704
Preprint. Discussion started: 6 September 2024

2 Data and methods

2.1 Data Sets

The North China Plain (NCP) encompasses 11 provinces and municipalities. We defined two regions of interest: the Northern NCP (NNCP) and the Southern NCP (SNCP). The NNCP region generally includes the cities of the Beijing-Tianjin-Hebei area, while the SNCP covers most areas south of the BTH region (**Figure 1**).

We utilized two types of air quality observations in this study. The first dataset consists of hourly air quality data released by the Ministry of Ecology and Environment of China since 2013. This dataset includes hourly PM2.5, O3, NO2, SO2 and CO concentrations from 823 national monitoring sites across 185 cities in the domain. Specifically, the NNCP contains 10 cities with 65 measurement sites, and the SNCP includes 24 cities with 95 sampling sites (**Figure 1**). The second dataset involves chemical compositions such as organic matter, nitrate, sulfate, and ammonium, observed at the Institute of Atmospheric Physics (IAP), Chinese Academy of Sciences in Beijing, China. Detailed descriptions of the methods used to obtain these chemical composition mass concentrations can be found in Sun et al. (2020).

We employed anthropogenic air pollutant emissions data for 2020 from mainland China, estimated using a bottom-up approach based on the near-real-time data (Zheng et al., 2021). The distributions of primary particles ($PM_{2.5}$) and gas pollutants (CO, SO_2, NOx, NH_3, and HCHO) reveal significantly higher emissions in the SNCP and the southern part of the NNCP region (**Figure S1**). These areas, characterized by lower elevations (**Figure 1**), exhibit higher emissions due to dense industrial and economic activities. Conversely, the northern part of the NNCP region, with higher elevations (**Figure 1**), shows relatively lower emissions.

The topographic characteristics of the NCP region, with higher elevations in the north and lower elevations in the south, combined with the high air pollutant emission areas in the south, suggest that under continuous southerly wind conditions, air pollutants can be readily transported northwards, potentially leading to severe haze events in the NNCP region.

https://doi.org/10.5194/egusphere-2024-2704
Preprint. Discussion started: 6 September 2024

2.2 WRF-Chem model description and configuration

We employed a specific version of the WRF-Chem model (Grell et al., 2005), simultaneously simulating gas precursors' emission, transport, mixing, and chemical transformation into particles and aerosols. Additionally, it considers cloud-aerosol interactions to trace the evolution of regional air quality. The model incorporates the CMAQ/Models-3 aerosol module (Binkowski and Roselle, 2003). Furthermore, it includes effects such as organic coating on nitrate formation by suppressing the N_2O_5 heterogeneous hydrolysis uptake(Liu et al., 2020b), the reaction of stabilized Criegee Intermediates (sCI) with SO_2 to form sulfate (Mauldin Iii et al., 2012), and a parameterization of sulfate heterogeneous formation from SO_2 involving Fe^{3+} catalyzed and irreversible uptake on aerosol liquid water surfaces (Li et al., 2017). Moreover, the Fast Tropospheric Ultraviolet and Visible (FTUV) radiation module calculates photolysis rates, and the model considers the interaction between aerosols and clouds (Li et al., 2011; Tie et al., 2003). Further details regarding this specific WRF-Chem model can be found in previous literature (Li et al., 2012). The WRF-Chem model has been utilized in numerous studies to simulate haze events(Feng et al., 2018; Liu et al., 2020b; Long et al., 2016), showcasing its proficiency in simulating $PM_{2.5}$ levels in China.

We simulated an unexpected air pollution event in the BTH region from January 21 to February 16, 2020. This event, characterized by elevated $PM_{2.5}$ levels, occurred despite a sudden reduction in anthropogenic emissions. The simulation domain, centred at (116° E, 38° N), consisted of a grid of 300 by 300 points, each spaced at a resolution of 6 km (**Figure 1**). In our base simulation (BASE), we utilized the anthropogenic air pollutant emission inventory of 2020(Zheng et al., 2021), along with meteorological initial and boundary conditions from NCEP FNL reanalysis data (Kalnay et al., 2018), alongside chemical initial and boundary conditions interpolated from MOZART 6-hour output(Horowitz et al., 2003). We computed the biogenic emissions online using the Model of Emissions of Gases and Aerosols from Nature (MEGAN). Integrated into the WRF-CHEM model, MEGAN generates net landscape-averaged biogenic emissions from terrestrial ecosystems into the above-canopy atmosphere, which are then used as inputs for further chemistry simulations(Guenther et al., 2006).

https://doi.org/10.5194/egusphere-2024-2704
Preprint. Discussion started: 6 September 2024

We also conducted two sensitivity simulations to investigate the impacts of emission decreases and meteorological variations on $PM_{2.5}$ levels (**Table 1**). The first simulation, called emission condition-sensitive simulation (SEN_EMIS), utilized the emission inventory from the BASE case but excluded any abrupt decreases (**Table S1 and Figure S2**) in anthropogenic emissions resulting from the lockdown (Huang et al., 2021), which allowed us to evaluate the comprehensive impact of sudden reductions in anthropogenic emissions on $PM_{2.5}$ levels. The second simulation, meteorology condition-sensitive simulation (SEN_METEO), averaged the climatology of NCEP FNL reanalysis data covering the period from 2015 to 2019 to represent varying meteorological initial and boundary conditions. By incorporating data from meteorological variations over multiple years, this approach provided a more stable reference point, thereby reducing the potential impact of anomalies or fluctuations in any single year's data, which allowed us to assess the comprehensive effect of meteorological factors on $PM_{2.5}$ levels.

3 Results and Discussions

3.1 Model performance

We assessed the model performance using several statistical parameters, including normalized mean bias (*NMB*), index of agreement (*IOA*), and correlation coefficient (*r*), to compare simulations against observational data. The evaluated variables encompass air pollutants such as $PM_{2.5}$, O_3, NO_2, SO_2, and CO concentrations within the NNCP and SNCP regions. PM2.5 components, including organic, nitrate, sulfate, and ammonium, are also assessed at the IAP monitoring site. These statistical metrics provide a quantitative measure of how well the model reproduces the observed data, offering insights into its accuracy and reliability in simulating the atmospheric conditions and pollutant levels during the specified period.

$$NMB = \frac{\sum_{i=1}^{N}(P_i - O_i)}{\sum_{i=1}^{N} O_i} \quad (1)$$

$$IOA = 1 - \frac{\sum_{i=1}^{N}(P_i - O_i)^2}{\sum_{i=1}^{N}(|P_i - \bar{O}| + |O_i - \bar{O}|)^2} \quad (2)$$

https://doi.org/10.5194/egusphere-2024-2704
Preprint. Discussion started: 6 September 2024

$$r = \frac{\sum_{i=1}^{N}(P_i-\overline{P})(O_i-\overline{O})}{\left[\sum_{i=1}^{N}(P_i-\overline{P})^2\sum_{i=1}^{N}(O_i-\overline{O})^2\right]^{\frac{1}{2}}} \quad (3)$$

where P_i and O_i represent the calculated and observed variables, respectively. N stands for the total number of predictions for comparison, and $\overline{O}$ and $\overline{P}$ denote the average observations and simulations, respectively. The *IOA* ranges from 0 to 1, where a value of 1 indicates perfect agreement between the predictions and observations. The *r* ranges from -1 to 1, 1 indicating perfect spatial consistency between the observations and predictions.

The temporal consistency between model simulations and observations is assessed using *NMB* and *IOA* (**Table 2 and Figures S3 and S4**). For $PM_{2.5}$ simulations, the average concentration in the NCP closely matched observations, with an *NMB* of −5.6% and an *IOA* of 0.91 in the NNCP, and an *NMB* of −2.1% and an *IOA* of 0.86 in the SNCP. For gaseous pollutants, such as SO_2, O_3, NO_2, and CO, the model effectively captured their diurnal concentration profiles in the NCP region, with *IOA*s exceeding 0.82 in the NNCP and 0.76 in the SNCP. The *NMB*s for these gaseous pollutants also showed good agreement with observations, with *IOAs* remaining below 6% in the NNCP and below 12% in the SNCP. The simulated mass concentrations of $PM_{2.5}$ components, including organic matter, nitrate, sulfate, and ammonium, at the IAP monitoring site, also effectively reproduced their temporal profiles of these chemical components, with *IOA*s exceeding 0.81. The model generally shows good agreement with observations for organic matter and nitrate, with *NMBs* of 15.0% and −18.9%, respectively, and *IOAs* exceeding 0.84. However, sulfate is significantly underestimated, with an *NMB* of −37.7%, which may be attributed to the model's incomplete representation of SO_2 oxidation pathways, particularly through heterogeneous chemistry during haze events (Zheng et al., 2015), and the acidic aerosol environment (Guo et al., 2017; Liu et al., 2017). Considering that SO_2, as the precursor of sulfate aerosols, is primarily emitted from point sources, such as power plants or industrial zones, the transport of SO_2 from these sources to the observation site is more sensitive to uncertainties in wind field simulation, causing significant fluctuations of SO_2 and the resultant simulated sulfate aerosols. This underestimation of sulfate also impacts ammonium concentrations (*NMB* = −23.6%), as ammonium is closely associated with sulfate and nitrate. Overall, while the model effectively captures the temporal variability of these components, the discrepancies in sulfate and ammonium suggest that further

https://doi.org/10.5194/egusphere-2024-2704
Preprint. Discussion started: 6 September 2024

improvements are needed, particularly in the representation of SO_2 emissions and associated chemical processes (Cheng et al., 2016; Li et al., 2018).

The correlation coefficient indicates the spatial consistency of model simulations compared to observations (**Figure 2**). During the episode, stagnant meteorological conditions with weak or calm winds led to unfavourable diffusion of atmospheric pollutants, accumulating and forming heavy haze pollution in the NCP region. The average simulated $PM_{2.5}$ mass concentrations exceeded 100 μg m^{-3} in the SNCP and exceeded 120 μg m^{-3} in the NNCP (**Figure 2a**). These results were consistent with observations, with a correlation coefficient 0.91 (**Figure 2e**). High O_3 levels exceeding 80 μg m^{-3} were simulated over the NNCP region (**Figure 2c**), which indicates an unexpectedly strong atmospheric oxidation capacity due to weakened titration from low NO_x emissions during the period. During the episode, almost all avoidable outdoor human activities and most transportation were prohibited. As a result, the average simulated NO_2 (**Figure 2b**) and SO_2 (**Figure 2d**) mass concentrations remained very low in the urban areas of NCP, with values below 30 μg m^{-3} and 10 μg m^{-3}, respectively. The spatial distributions of simulated and observed gaseous pollutants, averaged over the episode, also showed high spatial consistency, with correlation coefficients of 0.67 for O_3, 0.86 for SO_2, and 0.77 for NO_2 (**Figure 2e, 2f**).

The day-to-day variations also show good consistency between the observed and simulated concentrations of $PM_{2.5}$, O_3, NO_2, O_2, and CO (**Figure 3**). Despite some bias, the WRF-Chem model captures the temporal and spatial variations of $PM_{2.5}$ and gaseous air pollutants in the BTH region, which suggests that the emission inventory and simulated meteorological factors are generally reasonable, providing a reliable basis for further assessment.

3.2 Unexpected haze episodes in the NNCP

The COVID-19 pandemic lockdowns in China, which began in late January 2020, led to a sharp decline in socio-economic activities and a significant reduction in air pollutant emissions (Bao and Zhang, 2020; Liu et al., 2020a; Wang et al., 2020). In the NNCP, provincial emissions of NO_x, SO_2, and $PM_{2.5}$ decreased by 38-45%, 16-26%, and 12-18%, respectively(Huang et al., 2021). Observed concentrations of NO_2 and SO_2 significantly decreased to 30.8 μg m^{-3} and 13.5 μg m^{-3}, respectively(Li

https://doi.org/10.5194/egusphere-2024-2704
Preprint. Discussion started: 6 September 2024

et al., 2020; Zhao et al., 2020). Satellite observations from the TROPOMI instrument on Sentinel 5P captured a notable 65% reduction in column-integrated NO_2 over eastern China compared to the same period in 2019(Bauwens et al., 2020; Shi and Brasseur, 2020).

Despite the marked reduction in anthropogenic emissions and lower concentrations of NO_2 and SO_2, two unexpected heavy haze episodes, EP1 and EP2, occurred in the NNCP, respectively. During EP1, the average $PM_{2.5}$ concentration in the NNCP reached 153.4 μg m^{-3}, peaking at approximately 185 μg m^{-3}, significantly higher than in the SNCP, which peaked at around 120 μg m^{-3}. In EP2, the average $PM_{2.5}$ concentration in the NNCP reached 132.2 μg m^{-3}, peaking at approximately 150 μg m^{-3}. No haze was observed in SNNP during EP2, with average $PM_{2.5}$ concentrations of 57.7 μg m^{-3} (**Figure 3**).

During EP1, stagnant atmospheric conditions in the NNCP with wind speeds lower than 0.8 m s^{-1} (**Figures 4c, S5b, S5c**), coupled with a low planetary boundary layer height (PBLH) of approximately 306 m (ranging from 190 to 454 m) (**Figure S5a**), facilitated the accumulation of pollutants. Under these conditions, $PM_{2.5}$ concentrations (**Figure 3a**) reached peak values of around 150-200 μg m^{-3}, and O_3 concentrations (**Figure 3b**) steadily increased, peaking at approximately 90 μg m^{-3}. This trend indicates enhanced photochemical activity due to the stagnant conditions. Concurrently, NO_2 concentrations (**Figure 3c**) decreased, likely due to its conversion to O_3 and secondary aerosols. The consistently high levels of SO_2 and CO (**Figures 3d and 3e**) further indicated the limited dispersion under static atmospheric conditions. These conditions facilitated photochemical reactions, enhancing secondary pollution formation, as suggested by recent studies on secondary pollution during the COVID-19 lockdown(Huang et al., 2021).

In contrast, during EP2, the concentrations of $PM_{2.5}$, O_3, NO_2, SO_2, and CO (**Figure 2**) exhibited "∩" style fluctuating pattern, performing with the simultaneous increase and decrease of various pollutants. These fluctuating patterns indicate dynamic atmospheric conditions with significant air pollutant transport and mixing processes (**Figures 3d, S5b, S5c**). The northward speeds of about 4.1 m s^{-1} in the SNCP facilitated the transport of air pollutants from the SNCP to the NNCP. Simultaneously, stagnant atmospheric conditions in the NNCP with wind speeds lower than 0.5 m s^{-1}, corresponding with low PBLH of 306 m (ranging from 209 to 458 m) (**Figure S5a**), facilitated the accumulation of pollutants in the NNCP.

https://doi.org/10.5194/egusphere-2024-2704
Preprint. Discussion started: 6 September 2024

Overall, the contrasting atmospheric conditions during EP1 and EP2 underscore the complex interplay of meteorological factors and their significant impact on pollutant levels in the NNCP. The stagnant conditions during EP1 led to significant pollutant accumulation and secondary pollution formation, while the dynamic conditions during EP2 highlighted the role of regional pollutant transport in exacerbating haze episodes. These findings emphasize the need to consider local and regional atmospheric processes in air quality management strategies.

Reducing anthropogenic emissions has been a primary factor in decreasing $PM_{2.5}$ pollution in China(Bao and Zhang, 2020; Liu et al., 2020a). However, these haze episodes in NNCP during the COVID-19 lockdown challenge the relationship between human activities and air quality. These unexpected haze episodes underscore the complexity of air quality dynamics, suggesting that factors such as meteorological conditions, secondary pollutant formation, regional transport, and non-industrial sources also significantly impact air quality (Huang et al., 2021; Liu et al., 2020a; Shi and Brasseur, 2020). Future air quality management strategies must incorporate these multifaceted interactions for more effective pollution control.

3.3 Meteorological conditions increase the $PM_{2.5}$ in NNCP and decrease in SNCP

Meteorological factors significantly influence $PM_{2.5}$ concentrations throughout the study period (**Figure 5a**). $PM_{2.5}$ levels varied from -50 to 100 μg m^{-3}, exhibiting a distinct north-south disparity. In the NNCP, meteorological conditions lead to a notable increase in $PM_{2.5}$ levels, especially in the northern part, where concentrations exceed 50 to 100 μg m^{-3}. Conversely, the southern regions, particularly the western part of the SNCP, experienced a decrease in $PM_{2.5}$ levels, ranging from 30 to 50 μg m^{-3}. During haze episodes (EP1 and EP2), meteorological conditions induced a more significant absolute decrease in $PM_{2.5}$ in the NNCP compared to non-haze periods, with reductions of 5 to 30 μg m^{-3} (**Figure 5b**). These findings suggest that meteorological conditions were critical in exacerbating $PM_{2.5}$ pollution in the NNCP while mitigating it in the SNCP.

During the EP1 haze episode of January 22 to 29, 2020 (**Figure 5c**), meteorology conditions significantly increased $PM_{2.5}$ concentrations in the NNCP while decreasing them in the SNCP. During this period, the NNCP experienced stagnant surface winds (**Figure 4c**), and the lower PBLH in the

https://doi.org/10.5194/egusphere-2024-2704
Preprint. Discussion started: 6 September 2024

SEN_METEO case, which decreased by approximately 50 to 300 m on average compared to the BASE case (**Figure 6c**), deteriorated the dispersion of pollutants and further enhanced pollutant accumulation in the NNCP. In particular, in Beijing and surrounding areas, NO_2 concentrations showed a decreasing trend, likely due to its conversion to O_3 and secondary aerosols, combined with increased eastern winds, facilitated the accumulation of $PM_{2.5}$ in the northern NNCP, with period-average $PM_{2.5}$ increases exceeding 100 μg m^{-3} (**Figure 5c**). In contrast, the SNCP experienced a reduction in $PM_{2.5}$ levels with 30 to 50 μg m^{-3} (**Figure 5c**), possibly due to an increase in regional period-average PBLH by 50 to 300 m within the NNCP (**Figure 5c**), enhancing pollutant dispersion and dilution.

The effects of meteorology on $PM_{2.5}$ levels were more pronounced during EP2 compared to EP1 (**Figure 5c, 5d**). During the EP2 haze episode from February 8 to 13, 2020, meteorological conditions significantly exacerbated haze events in the NNCP while reducing $PM_{2.5}$ levels in the SNCP (**Figure 5d**). In the SEN_METEO case, the PBLH decreased by approximately 100 to 400 m on average in the NNCP, a larger drop than during EP1 (**Figure 6c, 6d**). Meanwhile, period-average northward wind speeds increased by about 3.0 to 5.0 m s^{-1} in the SNCP (**Figure 5d**), leading to continuous northward transport of $PM_{2.5}$ and its accumulation in the NNCP due to the blocking effects of the sudden rise in terrain (**Figure 1**). This process resulted in significant $PM_{2.5}$ increases, with large areas experiencing increases exceeding 100 to 200 μg m^{-3} in the NNCP. Conversely, the rise in PBLH and enhanced northward winds in the SNCP facilitated pollutant dispersion and dilution, resulting in a $PM_{2.5}$ decrease exceeding 30 to 50 μg m^{-3} in large areas of the SNCP (**Figure 5d**). The EP2 haze period highlighted the dominant role of atmospheric transport and mixing processes in exacerbating pollution, characterized by more dynamic atmospheric conditions, leading to simultaneous increases and decreases in various pollutant concentrations (**Figure 2**).

The near-surface temperature (T2) and relative humidity (RH) in the SEN_METEO case were higher than those in the BASE case, with the increase being more pronounced during the haze episodes of EP1 and EP2 (**Figures S6 and S7**). Elevated T2 can enhance atmospheric chemical reaction rates, subsequently facilitating the formation of secondary aerosols. Additionally, higher RH provides a favourable interface on aerosol surfaces, promoting heterogeneous reactions of particles. Previous studies have highlighted that abnormal meteorological conditions, characterized by higher T2 and RH

https://doi.org/10.5194/egusphere-2024-2704
Preprint. Discussion started: 6 September 2024

rather than emission reductions, dominated air pollution and enhanced secondary aerosol formation during the study period (Kong et al., 2023; Le et al., 2020; Ma et al., 2022).

3.4 Emission reduction decreases the $PM_{2.5}$ in the NSCP and SNCP

Abrupt decreases in anthropogenic emissions resulting from the lockdown period have significantly decreased $PM_{2.5}$ concentrations in the NSCP and SNCP (**Figure 7**). Both regions experienced substantial $PM_{2.5}$ reductions, leading to notable pollution alleviation. During haze episodes (EP1 and EP2), the absolute decrease in $PM_{2.5}$ was significantly higher than during non-haze periods. Specifically, $PM_{2.5}$ reductions during haze episodes generally exceeded 30 to 50 μg m^{-3}, compared to 5 to 30 μg m^{-3} during non-haze episodes (**Figure 7b, 7c, 7d**). This discrepancy underscores the enhanced effectiveness of emission control measures during these critical times.

In EP1, the reduction in $PM_{2.5}$ concentrations was amplified by low PBLH in the NNCP region. This meteorological condition intensified the effects of emission reductions, resulting in a more pronounced decrease in $PM_{2.5}$ levels ranging from 30 to 50 μg m^{-3} (**Figure 7c**). The wintertime O_3 production in urban areas of China operates in a NOx-saturated regime (NOx = NO + NO_2) due to the lack of HO_x radicals(Le et al., 2020; Seinfeld and Pandis, 2016). Reductions in NO emissions alleviate the daytime O_3 titration (Levy et al., 2014; Seinfeld and Pandis, 2016), leading to enhanced O_3 levels. Consequently, the O_3 enhancement in the NNCP during EP1 is primarily caused by the remarkable reductions of NOx. Previous studies, such as Huang et al. (2021), have emphasized that emission reductions can lead to unexpected air pollution by increasing secondary pollutants through enhanced atmospheric oxidation. Reductions in NOx emissions weaken ozone titration, leading to higher O_3 concentrations (Chang et al., 2020; Le et al., 2020; Lv et al., 2020; Shi and Brasseur, 2020).

During EP2, persistent northward pollution transport further highlighted the impact of emission reductions on the NNCP. The combined effects of local emission reductions and decreased atmospheric transport from the upwind SNCP region led to significant $PM_{2.5}$ decreases, particularly in areas along the mountain foothills where contributions exceeded 50 μg m^{-3} (**Figure 7d**). The results underscore the critical role of emission reductions in mitigating $PM_{2.5}$ pollution. During EP2 haze episodes, reductions lowered local $PM_{2.5}$ concentrations. They influenced regional pollutant transport patterns, highlighting

https://doi.org/10.5194/egusphere-2024-2704
Preprint. Discussion started: 6 September 2024

the necessity for coordinated emission control strategies across regions to maximize the reduction of $PM_{2.5}$ levels, especially under adverse meteorological conditions.

3.5 Combined effects of meteorology and emission reduction on $PM_{2.5}$

In the NNCP, meteorological conditions contributed to an increase in $PM_{2.5}$ levels (**Figure 6**). At the same time, emission reduction efforts decreased the $PM_{2.5}$ levels (**Figure 7**). The adverse impact of meteorological conditions often outweighs the benefits of emission reductions (**Figures 8 and 9a**). Specifically, during the entire simulation period, non-haze episode, EP1, and EP2, meteorological conditions caused regional $PM_{2.5}$ increases of 48.5 μg m^{-3}, 11.4 μg m^{-3}, 59.0 μg m^{-3}, and 108.8 μg m^{-3}, respectively. In contrast, emission reductions led to regional $PM_{2.5}$ decreases of 28.3 μg m^{-3}, 14.1 μg m^{-3}, 31.6 μg m^{-3}, and 52.2 μg m^{-3} for the same periods. Consequently, the combined effects of deteriorating meteorological conditions and emission reductions resulted in an overall increase of approximately 20 μg m^{-3} in $PM_{2.5}$ during the entire period in the NNCP, with more significant increases of 30 to 60 μg m^{-3} during EP1 and EP2, while during non-haze episodes, $PM_{2.5}$ slightly decreased by ~3 μg m^{-3}.

In contrast, the SNCP experienced a decrease in $PM_{2.5}$ due to both meteorological conditions and emission reductions (**Figure 8 and 9b**). During the entire period, non-haze period, EP1 and EP2, emission reductions caused $PM_{2.5}$ to decrease by 20 to 30 μg m^{-3}, while meteorological conditions led to decreases of 5 to 20 μg m^{-3}.

Overall, meteorological conditions tend to increase $PM_{2.5}$ in the NNCP and decrease it in the SNCP, while emission reductions consistently reduce $PM_{2.5}$ in both regions (**Figure S8**). Considering the combined effects of adverse meteorological conditions and mitigating emission reductions, $PM_{2.5}$ levels increased in the NNCP during the entire simulation period, particularly during EP1 and EP2, with regional episode-average $PM_{2.5}$ increases by 30 to 60 μg m^{-3}. Conversely, the SNCP exhibited a decrease in $PM_{2.5}$, ranging from approximately 20 to 40 μg m^{-3}.

4 Conclusions

This study highlights the significant but regionally variable impacts of meteorological conditions and emission reductions on $PM_{2.5}$ levels across the NCP during the COVID-19 lockdown. In the NNCP,

https://doi.org/10.5194/egusphere-2024-2704
Preprint. Discussion started: 6 September 2024

adverse meteorological conditions, characterized by cold, stagnant, and humid air masses, often outweighed the benefits of emission reductions, leading to increased $PM_{2.5}$ concentrations, especially during haze episodes. Conversely, in the SNCP, warmer air masses and more favourable meteorological conditions enhanced the effectiveness of emission reductions, resulting in decreased $PM_{2.5}$ levels.

Our findings underscore the critical role that meteorological conditions play in modulating the effects of emission reductions. The combination of unfavourable meteorological factors and emission reductions in the NNCP led to overall increases in $PM_{2.5}$ levels, with significant increases during haze episodes. Meanwhile, in the SNCP, meteorological conditions and emission reductions consistently contributed to lower $PM_{2.5}$ concentrations.

These results emphasize the necessity of integrated air quality management strategies for emission sources and atmospheric dynamics. By understanding the spatial and temporal variations in $PM_{2.5}$ in response to different meteorological conditions, policymakers can design more effective pollution control measures, particularly during critical pollution episodes. This study provides valuable insights into the complex interactions between emissions, meteorology, and air quality, highlighting the need for comprehensive approaches to improve air quality in the NCP.

Data availability

The code and data used in this study are from Xin Long (longxin@cigit.ac.cn).

Competing interests

The authors declare that they have no conflict of interest.

Author contribution

LL and XL designed the research and wrote the manuscript. YL, ZZ, YY, ZB, TF and JY contributed to interpreting the results. All the authors provided critical feedback and helped to improve the manuscript.

https://doi.org/10.5194/egusphere-2024-2704
Preprint. Discussion started: 6 September 2024

Acknowledgements

This work was supported by the National Natural Science Foundation of China (grant no. U23A2030, and 42007206), the Science and Technology Innovation Program of Hunan Province (2024AQ2004), the National University of Defense Technology Youth Independent Innovation Science Fund (ZK23-52), and the Open Fund of the State Key Laboratory of Loess and Quaternary Geology (grant no. SKLLQG2219). The authors also thank Tsinghua University for compiling and sharing the MEIC.

References

WHO (World Health Organisation): COVID-19 deaths, WHO COVID-19 Dashboard, World Health Organisation, https://data.who.int/dashboards/covid19/deaths?n=o, last access: 25 August 2024.

Bao, R. and Zhang, A.: Does lockdown reduce air pollution? Evidence from 44 cities in northern China, Sci. Total Environ., 731, 139052, 2020.

Bauwens, M., Compernolle, S., Stavrakou, T., Müller, J.-F., Van Gent, J., Eskes, H., Levelt, P. F., Van Der A, R., Veefkind, J. P., and Vlietinck, J.: Impact of coronavirus outbreak on NO2 pollution assessed using TROPOMI and OMI observations, Geophys. Res. Lett., 47, e2020GL087978, 2020.

Binkowski, F. S. and Roselle, S. J.: Models-3 community multiscale air quality (CMAQ) model aerosol component 1. Model description, J. Geophys. Res. Atmospheres, 108, 2003.

Chang, Y., Huang, R.-J., Ge, X., Huang, X., Hu, J., Duan, Y., Zou, Z., Liu, X., and Lehmann, M. F.: Puzzling haze events in China during the coronavirus (COVID-19) shutdown, Geophys. Res. Lett., 47, e2020GL088533, 2020.

Cheng, Y., Zheng, G., Wei, C., Mu, Q., Zheng, B., Wang, Z., Gao, M., Zhang, Q., He, K., and Carmichael, G.: Reactive nitrogen chemistry in aerosol water as a source of sulfate during haze events in China, Sci. Adv., 2, e1601530, 2016.

Ding, J., Dai, Q., Li, Y., Han, S., Zhang, Y., and Feng, Y.: Impact of meteorological condition changes on air quality and particulate chemical composition during the COVID-19 lockdown, J. Environ. Sci., 109, 45–56, 2021.

Dong, D. and Wang, J.: Air pollution as a substantial threat to the improvement of agricultural total factor productivity: Global evidence, Environ. Int., 173, 107842, 2023.

Feng, J., Liao, H., Li, Y., Zhang, Z., and Tang, Y.: Long-term trends and variations in haze-related weather conditions in north China during 1980–2018 based on emission-weighted stagnation intensity, Atmos. Environ., 240, 117830, 2020.

Feng, T., Bei, N., Zhao, S., Wu, J., Li, X., Zhang, T., Cao, J., Zhou, W., and Li, G.: Wintertime nitrate formation during haze days in the Guanzhong basin, China: A case study, Environ. Pollut., 243, 1057–1067, 2018.

Grell, G. A., Peckham, S. E., Schmitz, R., McKeen, S. A., Frost, G., Skamarock, W. C., and Eder, B.: Fully coupled "online" chemistry within the WRF model, Atmos. Environ., 39, 6957–6975, 2005.

https://doi.org/10.5194/egusphere-2024-2704
Preprint. Discussion started: 6 September 2024

Guenther, A., Karl, T., Harley, P., Wiedinmyer, C., Palmer, P. I., and Geron, C.: Estimates of global terrestrial isoprene emissions using MEGAN (Model of Emissions of Gases and Aerosols from Nature), Atmospheric Chem. Phys., 6, 3181–3210, 2006.

Guo, H., Liu, J., Froyd, K. D., Roberts, J. M., Veres, P. R., Hayes, P. L., Jimenez, J. L., Nenes, A., and Weber, R. J.: Fine particle pH and gas–particle phase partitioning of inorganic species in Pasadena, California, during the 2010 CalNex campaign, Atmospheric Chem. Phys., 17, 5703–5719, 2017.

Horowitz, L. W., Walters, S., Mauzerall, D. L., Emmons, L. K., Rasch, P. J., Granier, C., Tie, X., Lamarque, J.-F., Schultz, M. G., and Tyndall, G. S.: A global simulation of tropospheric ozone and related tracers: Description and evaluation of MOZART, version 2, J. Geophys. Res. Atmospheres, 108, 2003.

Huang, X., Ding, A., Gao, J., Zheng, B., Zhou, D., Qi, X., Tang, R., Wang, J., Ren, C., Nie, W., Chi, X., Xu, Z., Chen, L., Li, Y., Che, F., Pang, N., Wang, H., Tong, D., Qin, W., Cheng, W., Liu, W., Fu, Q., Liu, B., Chai, F., Davis, S. J., Zhang, Q., and He, K.: Enhanced secondary pollution offset reduction of primary emissions during COVID-19 lockdown in China, Natl. Sci. Rev., 8, nwaa137, https://doi.org/10.1093/nsr/nwaa137, 2021.

Kalnay, E., Kanamitsu, M., Kistler, R., Collins, W., Deaven, D., Gandin, L., Iredell, M., Saha, S., White, G., and Woollen, J.: The NCEP/NCAR 40-year reanalysis project, in: Renewable energy, Routledge, Vol1_146-Vol1_194, 2018.

Kong, L., Tang, X., Zhu, J., Wang, Z., Sun, Y., Fu, P., Gao, M., Wu, H., Lu, M., and Wu, Q.: Unbalanced emission reductions of different species and sectors in China during COVID-19 lockdown derived by multi-species surface observation assimilation, Atmospheric Chem. Phys., 23, 6217–6240, 2023.

Le, T., Wang, Y., Liu, L., Yang, J., Yung, Y. L., Li, G., and Seinfeld, J. H.: Unexpected air pollution with marked emission reductions during the COVID-19 outbreak in China, Science, 369, 702–706, 2020.

Lelieveld, J., Haines, A., and Pozzer, A.: Age-dependent health risk from ambient air pollution: a modelling and data analysis of childhood mortality in middle-income and low-income countries, Lancet Planet. Health, 2, e292–e300, 2018.

Levy, I., Mihele, C., Lu, G., Narayan, J., and Brook, J. R.: Evaluating multipollutant exposure and urban air quality: pollutant interrelationships, neighborhood variability, and nitrogen dioxide as a proxy pollutant, Environ. Health Perspect., 122, 65–72, 2014.

Li, G., Bei, N., Tie, X., and Molina, L. T.: Aerosol effects on the photochemistry in Mexico City during MCMA-2006/MILAGRO campaign, Atmospheric Chem. Phys., 11, 5169–5182, 2011.

Li, G., Lei, W., Bei, N., and Molina, L. T.: Contribution of garbage burning to chloride and PM 2.5 in Mexico City, Atmospheric Chem. Phys., 12, 8751–8761, 2012.

Li, G., Bei, N., Cao, J., Huang, R., Wu, J., Feng, T., Wang, Y., Liu, S., Zhang, Q., and Tie, X.: A possible pathway for rapid growth of sulfate during haze days in China, Atmospheric Chem. Phys., 17, 3301–3316, 2017.

Li, J., Liao, H., Hu, J., and Li, N.: Severe particulate pollution days in China during 2013–2018 and the associated typical weather patterns in Beijing-Tianjin-Hebei and the Yangtze River Delta regions, Environ. Pollut., 248, 74–81, 2019.

https://doi.org/10.5194/egusphere-2024-2704
Preprint. Discussion started: 6 September 2024

Li, J., Gao, W., Cao, L., He, L., Zhang, X., Yan, Y., Mao, J., Xin, J., Wang, L., and Tang, G.: Effects of different stagnant meteorological conditions on aerosol chemistry and regional transport changes in Beijing, China, Atmos. Environ., 258, 118483, 2021.

Li, J., Carlson, B. E., Yung, Y. L., Lv, D., Hansen, J., Penner, J. E., Liao, H., Ramaswamy, V., Kahn, R. A., and Zhang, P.: Scattering and absorbing aerosols in the climate system, Nat. Rev. Earth Environ., 3, 363–379, 2022.

Li, L., Hoffmann, M. R., and Colussi, A. J.: Role of nitrogen dioxide in the production of sulfate during Chinese haze-aerosol episodes, Environ. Sci. Technol., 52, 2686–2693, 2018.

Li, L., Li, Q., Huang, L., Wang, Q., Zhu, A., Xu, J., Liu, Z., Li, H., Shi, L., and Li, R.: Air quality changes during the COVID-19 lockdown over the Yangtze River Delta Region: An insight into the impact of human activity pattern changes on air pollution variation, Sci. Total Environ., 732, 139282, 2020.

Liu, F., Page, A., Strode, S. A., Yoshida, Y., Choi, S., Zheng, B., Lamsal, L. N., Li, C., Krotkov, N. A., and Eskes, H.: Abrupt decline in tropospheric nitrogen dioxide over China after the outbreak of COVID-19, Sci. Adv., 6, eabc2992, 2020a.

Liu, L., Bei, N., Hu, B., Wu, J., Liu, S., Li, X., Wang, R., Liu, Z., Shen, Z., and Li, G.: Wintertime nitrate formation pathways in the north China plain: Importance of N2O5 heterogeneous hydrolysis, Environ. Pollut., 266, 115287, 2020b.

Liu, M., Song, Y., Zhou, T., Xu, Z., Yan, C., Zheng, M., Wu, Z., Hu, M., Wu, Y., and Zhu, T.: Fine particle pH during severe haze episodes in northern China, Geophys. Res. Lett., 44, 5213–5221, 2017.

Liu, Y., Wang, T., Stavrakou, T., Elguindi, N., Doumbia, T., Granier, C., Bouarar, I., Gaubert, B., and Brasseur, G. P.: Diverse response of surface ozone to COVID-19 lockdown in China, Sci. Total Environ., 789, 147739, 2021.

Long, X., Tie, X., Cao, J., Huang, R., Feng, T., Li, N., Zhao, S., Tian, J., Li, G., and Zhang, Q.: Impact of crop field burning and mountains on heavy haze in the North China Plain: a case study, Atmospheric Chem. Phys., 16, 9675–9691, 2016.

Lv, Z., Wang, X., Deng, F., Ying, Q., Archibald, A. T., Jones, R. L., Ding, Y., Cheng, Y., Fu, M., and Liu, Y.: Source–receptor relationship revealed by the halted traffic and aggravated haze in Beijing during the COVID-19 lockdown, Environ. Sci. Technol., 54, 15660–15670, 2020.

Ma, T., Duan, F., Ma, Y., Zhang, Q., Xu, Y., Li, W., Zhu, L., and He, K.: Unbalanced emission reductions and adverse meteorological conditions facilitate the formation of secondary pollutants during the COVID-19 lockdown in Beijing, Sci. Total Environ., 838, 155970, 2022.

Mauldin Iii, R. L., Berndt, T., Sipilä, M., Paasonen, P., Petäjä, T., Kim, S., Kurtén, T., Stratmann, F., Kerminen, V.-M., and Kulmala, M.: A new atmospherically relevant oxidant of sulphur dioxide, Nature, 488, 193–196, 2012.

Seinfeld, J. H. and Pandis, S. N.: Atmospheric chemistry and physics: from air pollution to climate change, John Wiley & Sons, 2016.

Shen, F., Hegglin, M. I., and Yuan, Y.: Impact of weather patterns and meteorological factors on PM 2.5 and O 3 responses to the COVID-19 lockdown in China, Atmospheric Chem. Phys., 24, 6539–6553, 2024.

https://doi.org/10.5194/egusphere-2024-2704
Preprint. Discussion started: 6 September 2024

Shi, X. and Brasseur, G. P.: The response in air quality to the reduction of Chinese economic activities during the COVID-19 outbreak, Geophys. Res. Lett., 47, e2020GL088070, 2020.

Su, T., Li, Z., Zheng, Y., Luan, Q., and Guo, J.: Abnormally Shallow Boundary Layer Associated With Severe Air Pollution During the COVID-19 Lockdown in China, Geophys. Res. Lett., 47, e2020GL090041, https://doi.org/10.1029/2020GL090041, 2020.

Sun, Y., Lei, L., Zhou, W., Chen, C., He, Y., Sun, J., Li, Z., Xu, W., Wang, Q., and Ji, D.: A chemical cocktail during the COVID-19 outbreak in Beijing, China: Insights from six-year aerosol particle composition measurements during the Chinese New Year holiday, Sci. Total Environ., 742, 140739, 2020.

Tie, X., Madronich, S., Walters, S., Zhang, R., Rasch, P., and Collins, W.: Effect of clouds on photolysis and oxidants in the troposphere, J. Geophys. Res. Atmospheres, 108, 2003.

Wang, C., Horby, P. W., Hayden, F. G., and Gao, G. F.: A novel coronavirus outbreak of global health concern, The lancet, 395, 470–473, 2020.

Wang, J., Lei, Y., Chen, Y., Wu, Y., Ge, X., Shen, F., Zhang, J., Ye, J., Nie, D., and Zhao, X.: Comparison of air pollutants and their health effects in two developed regions in China during the COVID-19 pandemic, J. Environ. Manage., 287, 112296, 2021.

Xiao, Q., Geng, G., Liang, F., Wang, X., Lv, Z., Lei, Y., Huang, X., Zhang, Q., Liu, Y., and He, K.: Changes in spatial patterns of PM2. 5 pollution in China 2000–2018: Impact of clean air policies, Environ. Int., 141, 105776, 2020.

Xu, J., Ge, X., Zhang, X., Zhao, W., Zhang, R., and Zhang, Y.: COVID-19 impact on the concentration and composition of submicron particulate matter in a typical city of Northwest China, Geophys. Res. Lett., 47, e2020GL089035, 2020.

Yang, G., Ren, G., Zhang, P., Xue, X., Tysa, S. K., Jia, W., Qin, Y., Zheng, X., and Zhang, S.: PM2. 5 influence on urban heat island (UHI) effect in Beijing and the possible mechanisms, J. Geophys. Res. Atmospheres, 126, e2021JD035227, 2021.

Zhang, Q., Zheng, Y., Tong, D., Shao, M., Wang, S., Zhang, Y., Xu, X., Wang, J., He, H., and Liu, W.: Drivers of improved PM2. 5 air quality in China from 2013 to 2017, Proc. Natl. Acad. Sci., 116, 24463–24469, 2019.

Zhao, Y., Zhang, K., Xu, X., Shen, H., Zhu, X., Zhang, Y., Hu, Y., and Shen, G.: Substantial Changes in Nitrogen Dioxide and Ozone after Excluding Meteorological Impacts during the COVID-19 Outbreak in Mainland China, Environ. Sci. Technol. Lett., 7, 402–408, https://doi.org/10.1021/acs.estlett.0c00304, 2020.

Zheng, B., Zhang, Q., Geng, G., Chen, C., Shi, Q., Cui, M., Lei, Y., and He, K.: Changes in China's anthropogenic emissions and air quality during the COVID-19 pandemic in 2020, Earth Syst. Sci. Data, 13, 2895–2907, 2021.

Zheng, G. J., Duan, F. K., Su, H., Ma, Y. L., Cheng, Y., Zheng, B., Zhang, Q., Huang, T., Kimoto, T., Chang, D., Pöschl, U., Cheng, Y. F., and He, K. B.: Exploring the severe winter haze in Beijing: the impact of synoptic weather, regional transport and heterogeneous reactions, Atmospheric Chem. Phys., 15, 2969–2983, https://doi.org/10.5194/acp-15-2969-2015, 2015.

https://doi.org/10.5194/egusphere-2024-2704
Preprint. Discussion started: 6 September 2024

Figure Captions

Figure 1. The simulation domain in WRF-Chem, including topography. Circles represent the locations of cities with ambient air quality monitoring sites, and the size of each circle corresponds to the number of monitoring sites in that city. The regions of interest, NNCP (Northern North China Plain) and SNCP (Southern North China Plain), are highlighted.

Figure 2. The pattern comparisons between average observations and simulations for (a) $PM_{2.5}$, (b) SO_2, (c) O_3, and (d) NO_2, along with the simulated surface wind fields during the period. Additionally, statistical comparisons are presented for (e) $PM_{2.5}$ and O_3, and (f) SO_2 and NO_2, along with their correlation coefficients (*r*).

Figure 3. Observed (solid lines) and simulated (dashed lines) day-to-day variations in surface $PM_{2.5}$ O_3, NO_2, SO_2, and CO levels in the NNCP (red lines) and SNCP (blue lines) from January 21 to February 15, 2020. The daily concentrations of the pollutants were calculated from the 24-hour averages, except for O_3, which was calculated from the 10:00 to 17:00 averages. Two haze episodes occurred during the study period: EP1 from January 22 to 29, and EP2 from February 8 to 13.

Figure 4. The spatial patterns of near-surface simulated $PM_{2.5}$ averaged from (a) the entire study period, (b) the non-haze period, (c) the EP1 haze period, and (d) the EP2 haze period, along with the simulated surface wind fields.

Figure 5. The pattern comparisons between the "BASE" and "SEN_METEO" simulations. The color gradient represents $PM_{2.5}$ changes averaged from (a) the entire study period, (b) the non-haze period, (c) the EP1 haze period, and (d) the EP2 haze period, along with the simulated surface wind fields.

Figure 6. The pattern comparisons between the "BASE" and "SEN_METEO" simulations. The color gradient represents PBLH changes averaged from (a) the entire study period, (b) the non-haze period, (c) the EP1 haze period, and (d) the EP2 haze period.

Figure 7. The pattern comparisons between the "BASE" and "SEN_ EMIS" simulations. The color gradient represents $PM_{2.5}$ changes averaged from (a) the entire study period, (b) the non-haze period, (c) the EP1 haze period, and (d) the EP2 haze period.

Figure 8. Comparisons of $PM_{2.5}$ changes combining the impacts of "SEN_METEO" and "SEN_ EMIS" cases. The color gradient represents $PM_{2.5}$ changes averaged from (a) the entire study period, (b) the non-haze period, (c) the EP1 haze period, and (d) the EP2 haze period.

Figure 9. Regional contributions to $PM_{2.5}$ averaged in (a) the NNCP and (b) the SNCP during the entire period, non-haze period, EP1, and EP2. The contributions include meteorological conditions (METEO), abrupt decreases in anthropogenic emissions (EMIS), and combined effects of METEO and EMIS (Combined).

https://doi.org/10.5194/egusphere-2024-2704
Preprint. Discussion started: 6 September 2024

Table Captions

Table 1 Configurations of simulation cases in this study

Table 2. The statistical parameters of model performance include temporal assessments of *MB*, and *IOA* in the NNCP and SCNP and at the IAP monitoring site.

https://doi.org/10.5194/egusphere-2024-2704
Preprint. Discussion started: 6 September 2024

Figure 1

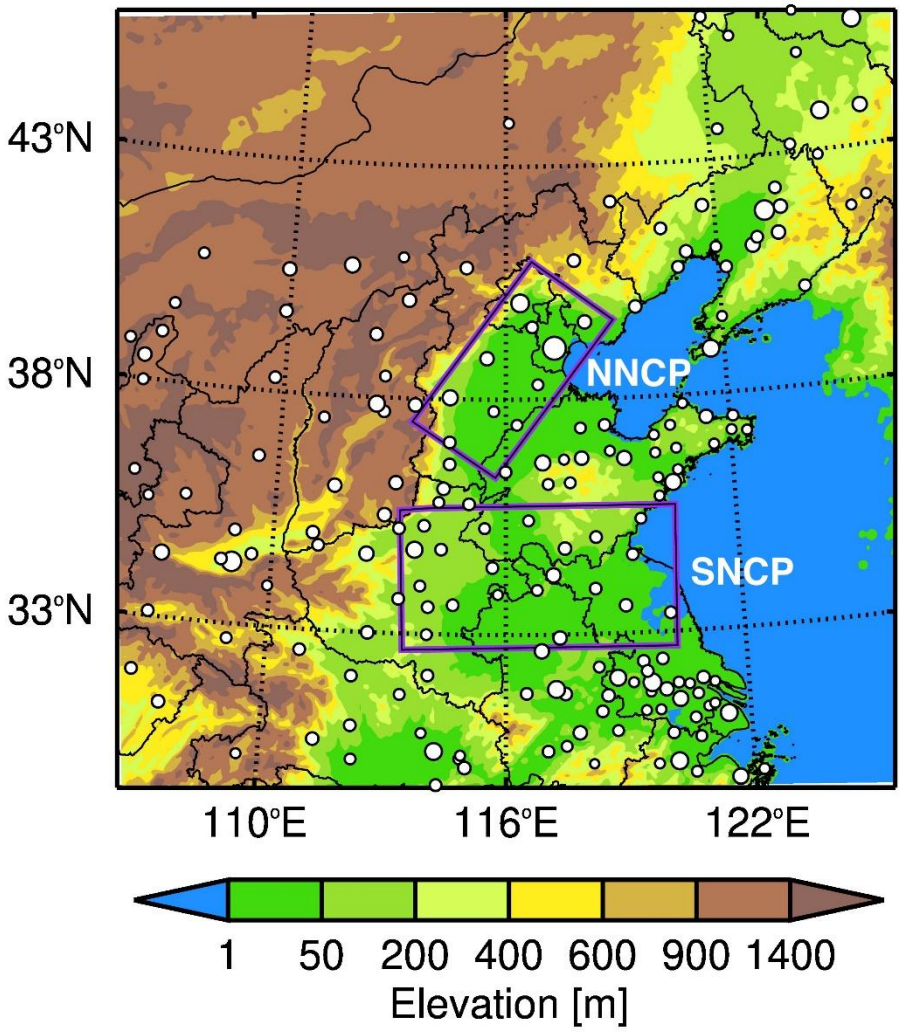

Figure 1. The simulation domain in WRF-Chem, including topography. Circles represent the locations of cities with ambient air quality monitoring sites, and the size of each circle corresponds to the number of monitoring sites in that city. The regions of interest, NNCP (Northern North China Plain) and SNCP (Southern North China Plain), are highlighted.

https://doi.org/10.5194/egusphere-2024-2704
Preprint. Discussion started: 6 September 2024

Figure 2

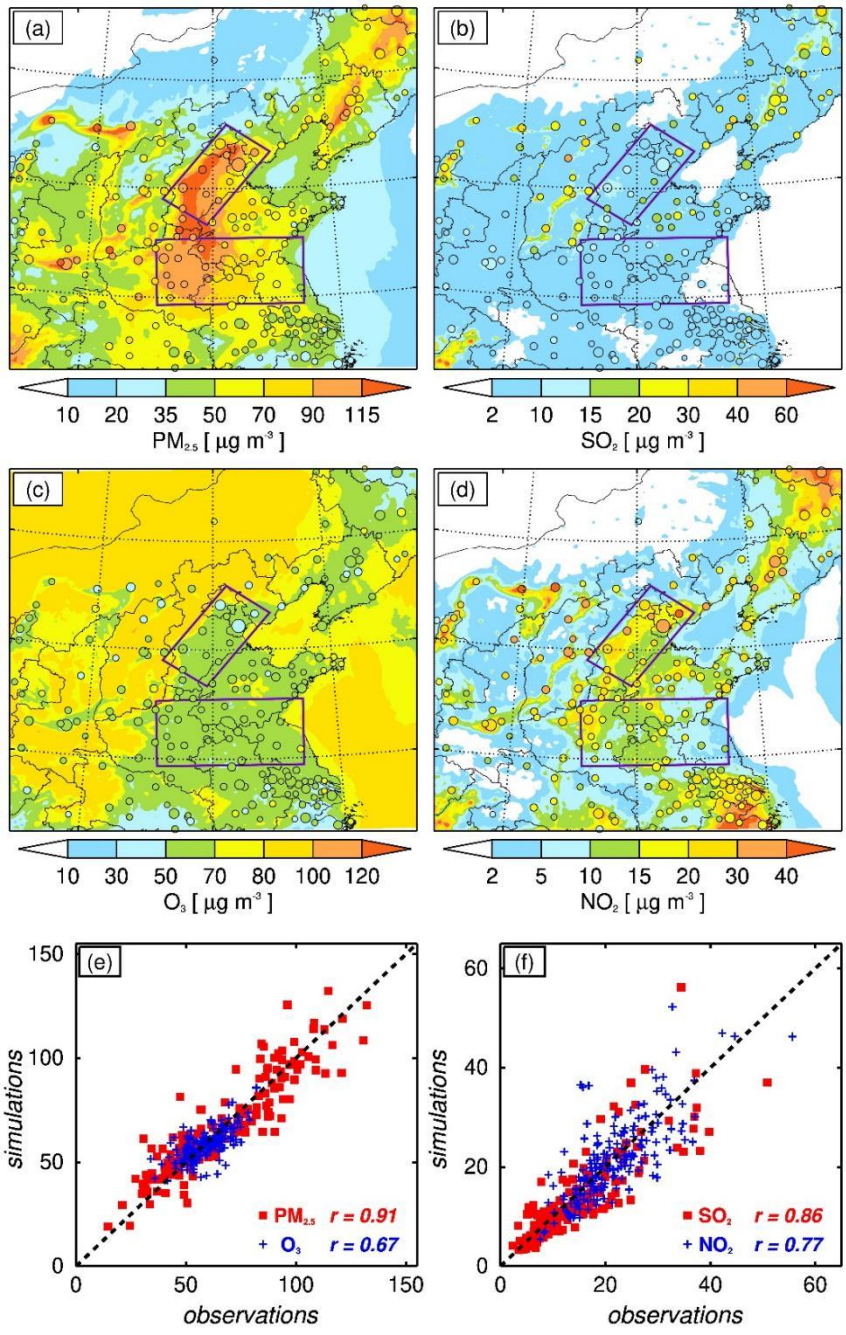

Figure 2. The pattern comparisons between average observations and simulations for (a) $PM_{2.5}$, (b) SO_2, (c) O_3, and (d) NO_2, along with the simulated surface wind fields during the period. Additionally, statistical comparisons are presented for (e) $PM_{2.5}$ and O_3, and (f) SO_2 and NO_2, along with their correlation coefficients (*r*).

https://doi.org/10.5194/egusphere-2024-2704
Preprint. Discussion started: 6 September 2024

Figure 3

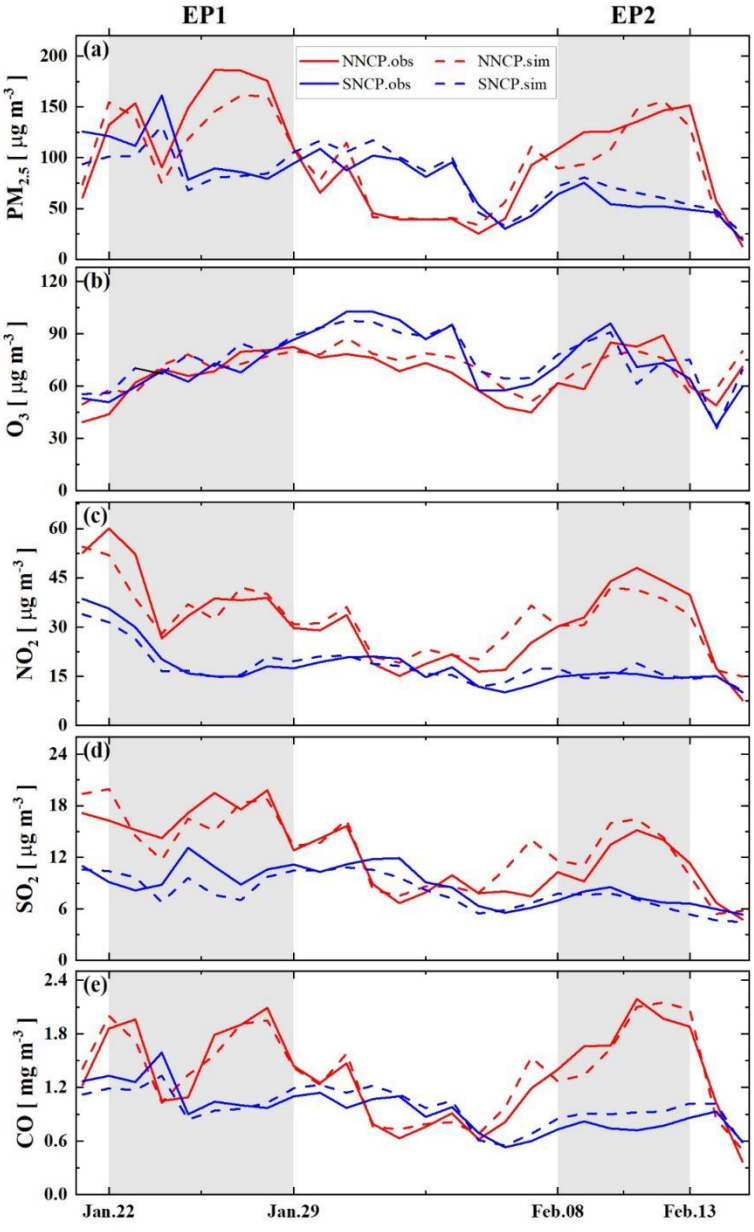

Figure 3. Observed (solid lines) and simulated (dashed lines) day-to-day variations in surface $PM_{2.5}$ O_3, NO_2, SO_2, and CO levels in the NNCP (red lines) and SNCP (blue lines) from January 21 to February 15, 2020. The daily concentrations of the pollutants were calculated from the 24-hour averages, except for O_3, which was calculated from the 10:00 to 17:00 averages. Two haze episodes occurred during the study period: EP1 from January 22 to 29, and EP2 from February 8 to 13.

https://doi.org/10.5194/egusphere-2024-2704
Preprint. Discussion started: 6 September 2024

Figure 4

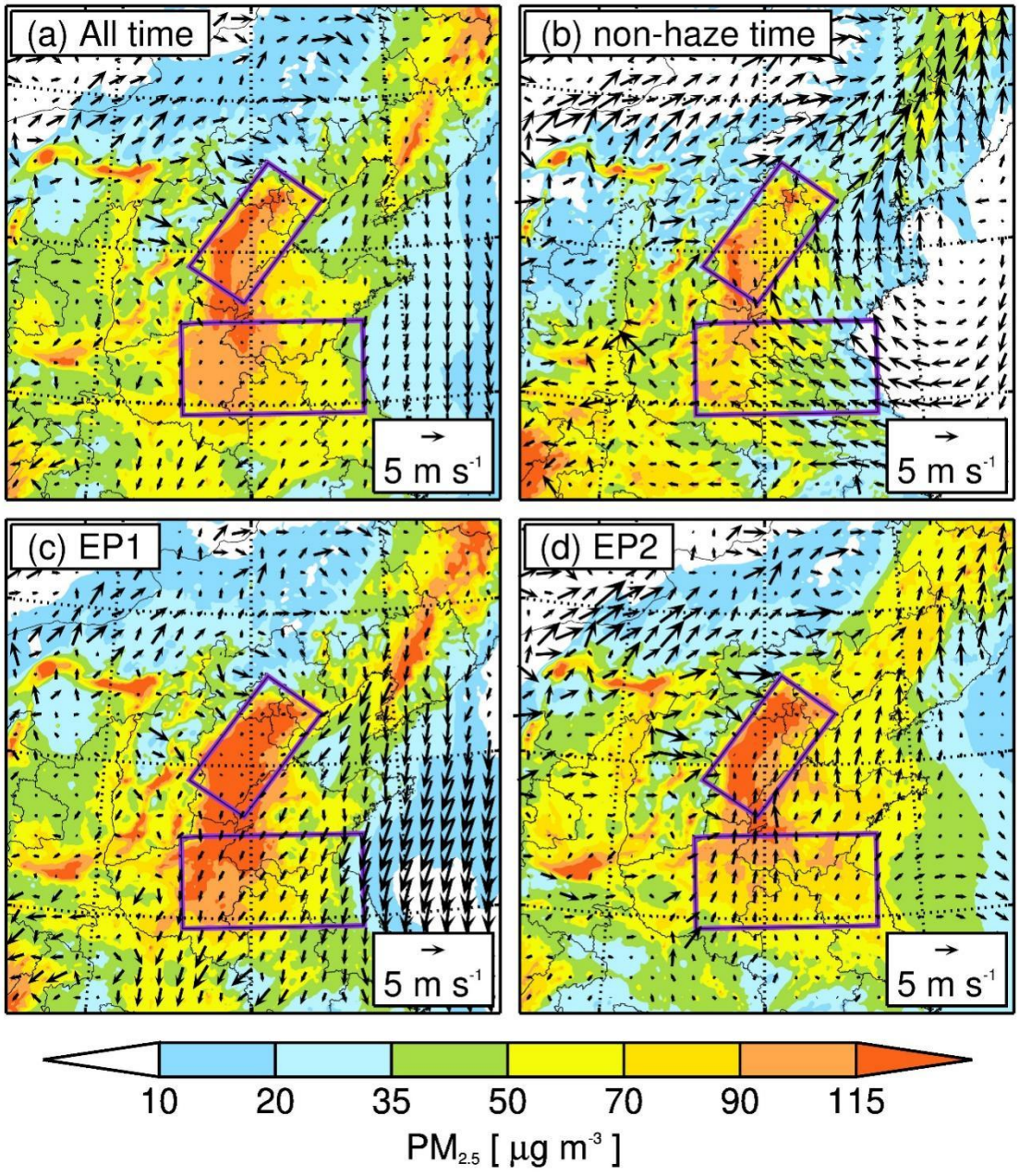

Figure 4. The spatial patterns of near-surface simulated $PM_{2.5}$ averaged from (a) the entire study period, (b) the non-haze period, (c) the EP1 haze period, and (d) the EP2 haze period, along with the simulated surface wind fields.

https://doi.org/10.5194/egusphere-2024-2704
Preprint. Discussion started: 6 September 2024

Figure 5

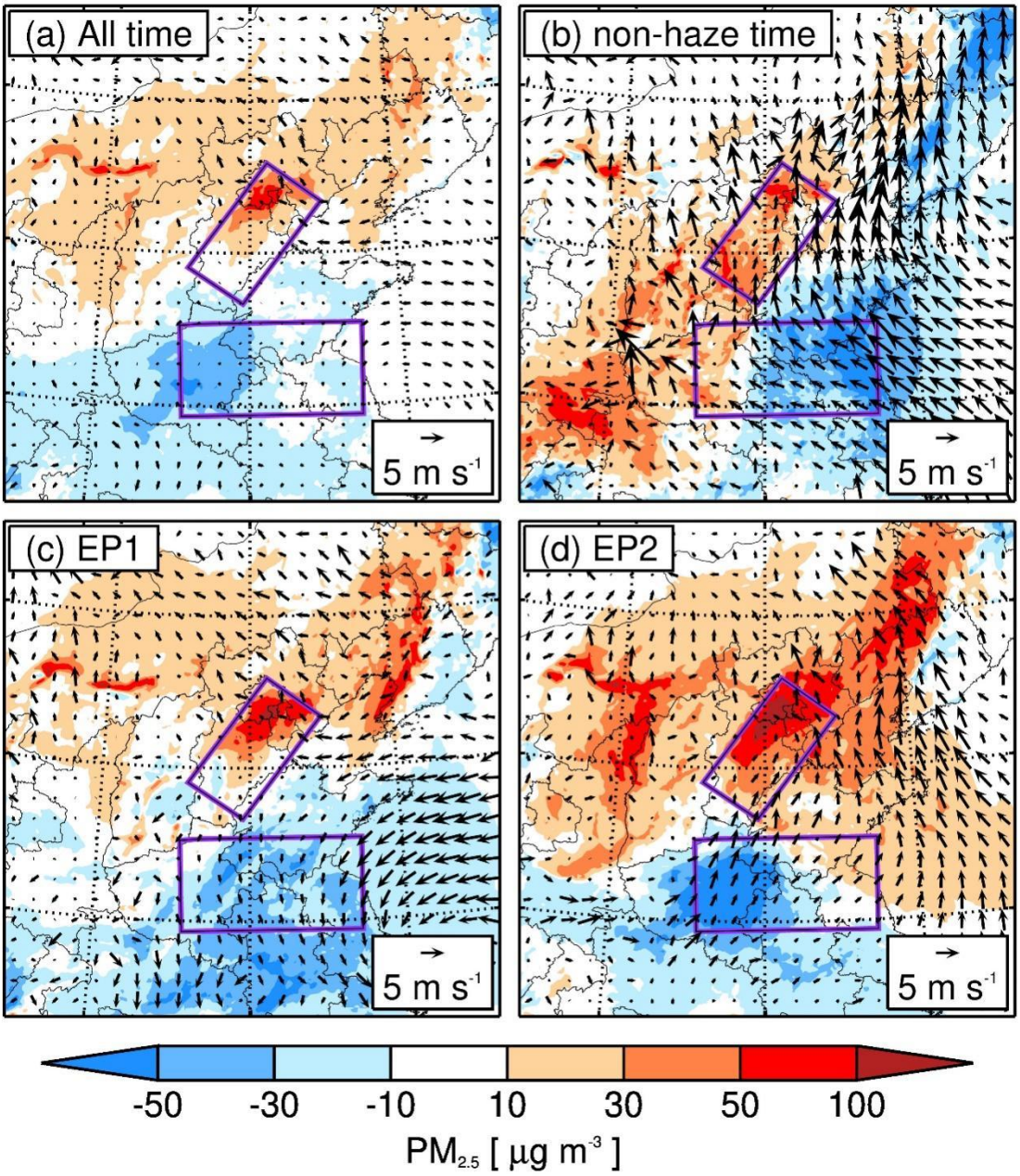

Figure 5. The pattern comparisons between the "BASE" and "SEN_METEO" simulations. The color gradient represents $PM_{2.5}$ changes averaged from (a) the entire study period, (b) the non-haze period, (c) the EP1 haze period, and (d) the EP2 haze period, along with the simulated surface wind fields.

https://doi.org/10.5194/egusphere-2024-2704
Preprint. Discussion started: 6 September 2024

Figure 6

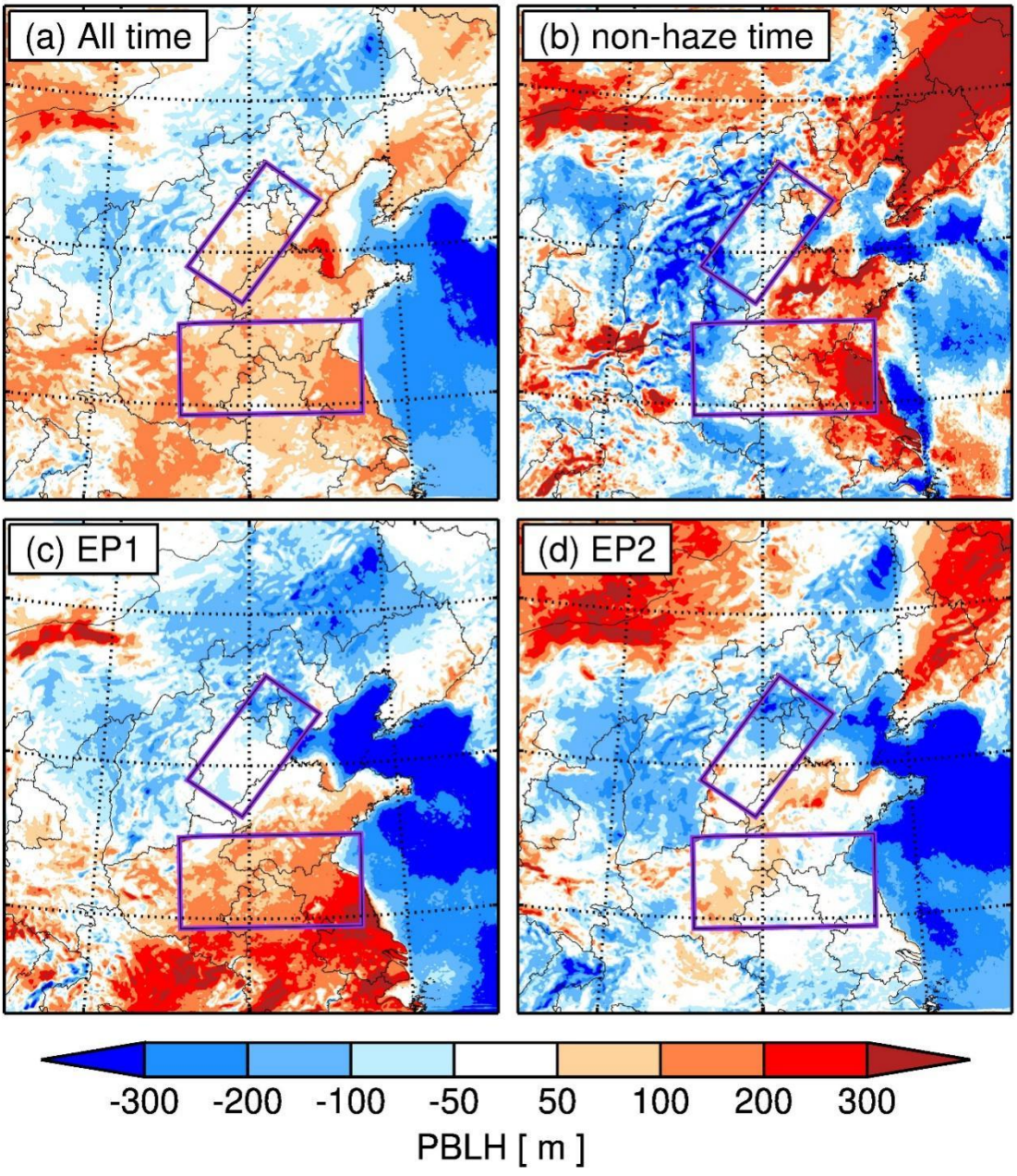

Figure 6. The pattern comparisons between the "BASE" and "SEN_METEO" simulations. The color gradient represents PBLH changes averaged from (a) the entire study period, (b) the non-haze period, (c) the EP1 haze period, and (d) the EP2 haze period.

https://doi.org/10.5194/egusphere-2024-2704
Preprint. Discussion started: 6 September 2024

Figure 7

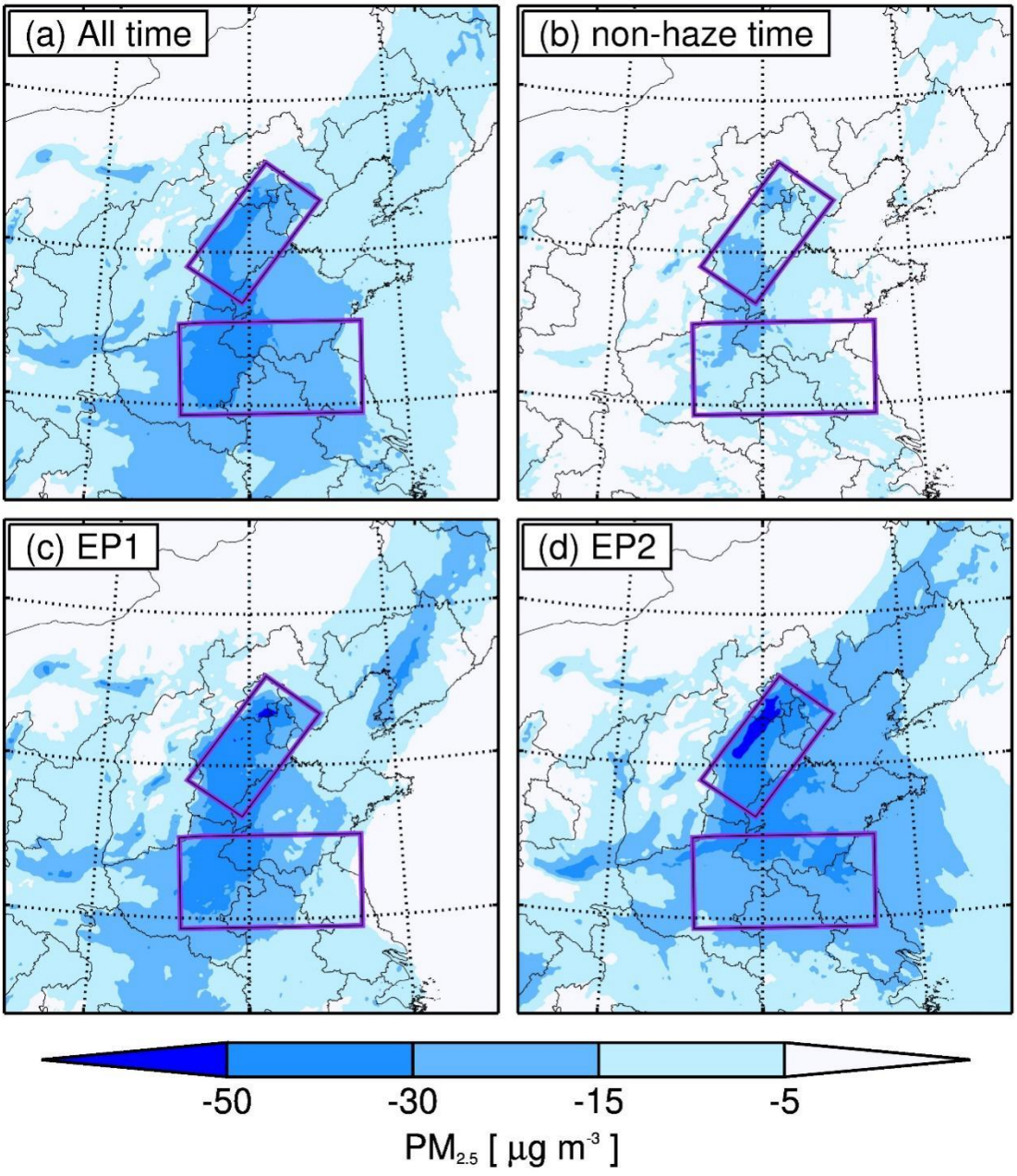

Figure 7. The pattern comparisons between the "BASE" and "SEN_ EMIS" simulations. The color gradient represents $PM_{2.5}$ changes averaged from (a) the entire study period, (b) the non-haze period, (c) the EP1 haze period, and (d) the EP2 haze period.

https://doi.org/10.5194/egusphere-2024-2704
Preprint. Discussion started: 6 September 2024

Figure 8

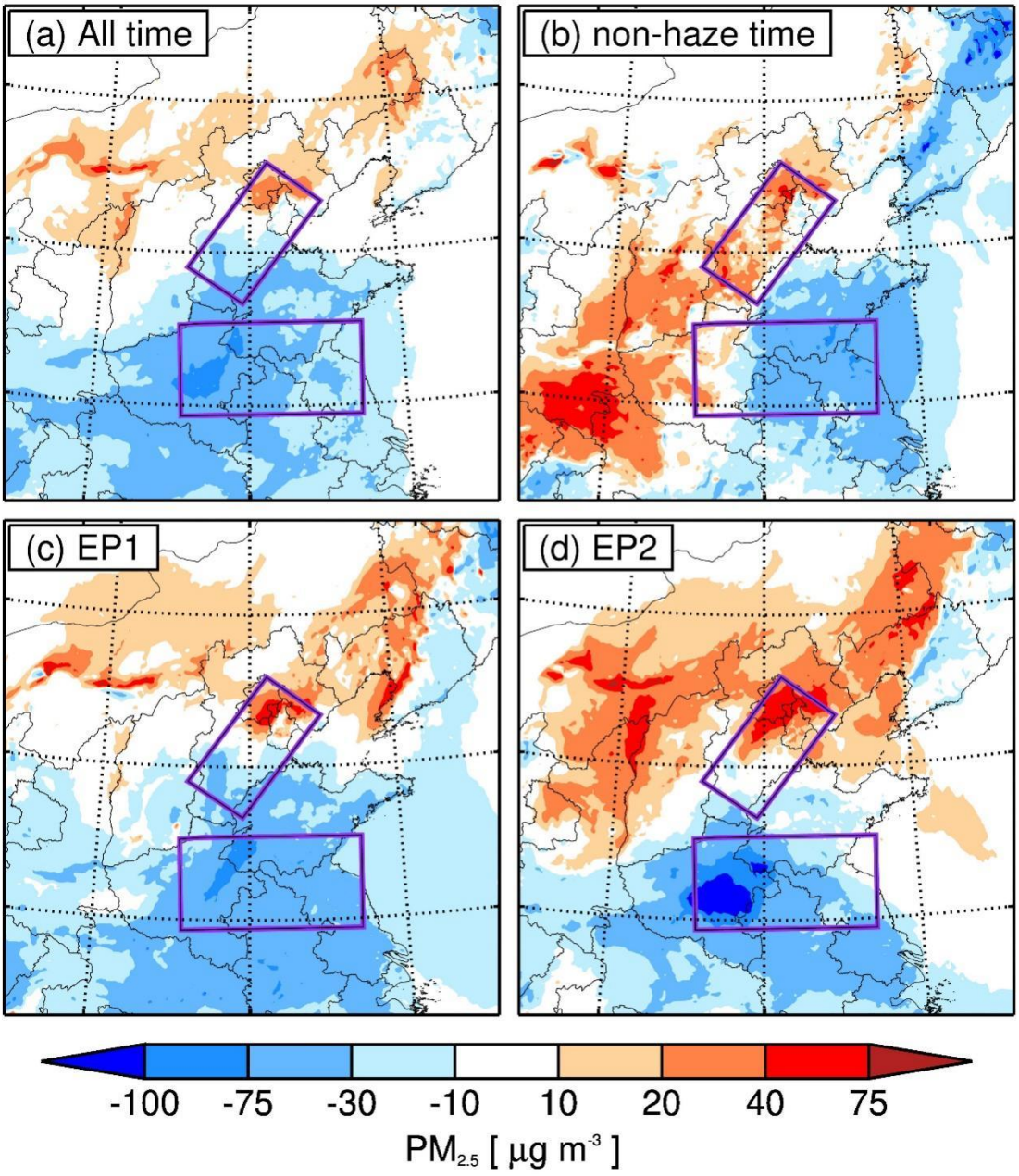

Figure 8. Comparisons of $PM_{2.5}$ changes combining the impacts of "SEN_METEO" and "SEN_ EMIS" cases. The color gradient represents $PM_{2.5}$ changes averaged from (a) the entire study period, (b) the non-haze period, (c) the EP1 haze period, and (d) the EP2 haze period.

https://doi.org/10.5194/egusphere-2024-2704
Preprint. Discussion started: 6 September 2024

Figure 9

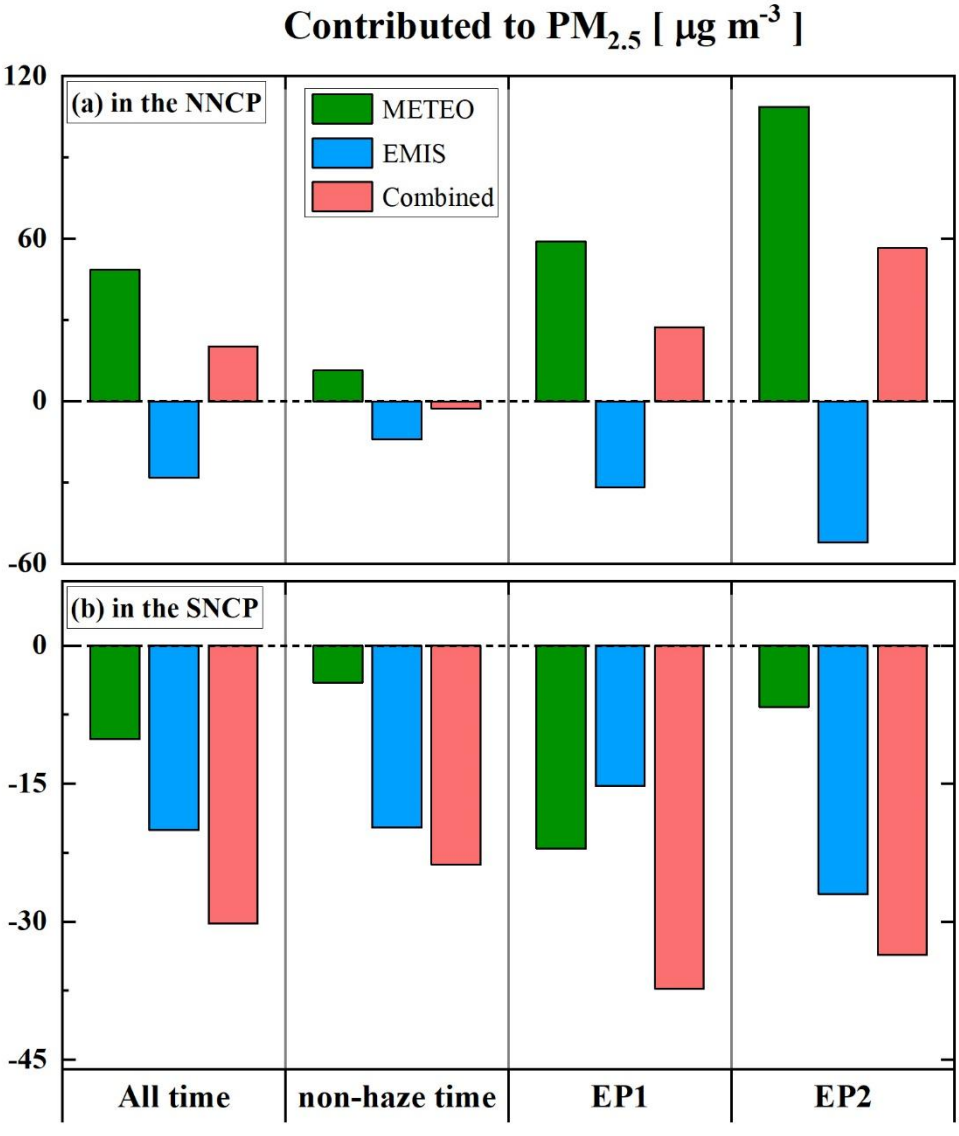

Figure 9. Regional contributions to $PM_{2.5}$ averaged in (a) the NNCP and (b) the SNCP during the entire period, non-haze period, EP1, and EP2. The contributions include meteorological conditions (METEO), abrupt decreases in anthropogenic emissions (EMIS), and combined effects of METEO and EMIS (Combined).

https://doi.org/10.5194/egusphere-2024-2704
Preprint. Discussion started: 6 September 2024

Table 1

Table 1 Configurations of simulation cases in this study

Experiments	The year of anthropogenic emission inventory	The year of meteorological initial and boundary conditions
BASE	**2020**	**2020**
Sen_2015	2020	2015
Sen_2016	2020	2016
Sen_2017	2020	2017
Sen_2018	2020	2018
Sen_2019	2020	2019
SEN_METEO	**2020**	**Average from 2015 to 2019**
SEN_EMIS	**2019**	**2020**

https://doi.org/10.5194/egusphere-2024-2704
Preprint. Discussion started: 6 September 2024

Table 2

Table 2. The statistical parameters of model performance include temporal assessments of *MB*, and *IOA* in the NNCP and SCNP and at the IAP monitoring site.

Statistical parameters	*NMB*	*IOA*
In the NNCP region		
$PM_{2.5}$	−5.6%	0.91
SO_2	4.8%	0.82
O_3	4.4%	0.86
NO_2	2.3%	0.82
CO	1.5%	0.85
In the SNCP region		
$PM_{2.5}$	−2.1%	0.86
SO_2	−11.0%	0.76
O_3	−10.2%	0.88
NO_2	0.1%	0.87
CO	6.0%	0.79
At the IAP monitoring site		
Organic	15.0%	0.84
Nitrate	−18.9%	0.88
Sulfate	−37.7%	0.81
Ammonium	−23.6%	0.87